J|A|C|S
ARTICLES
Published on Web 06/18/2005

Synthesis and Magnetic Properties Comparison of M−Cu(II) and M−VO(II) Schiff Base−Porphyrazine Complexes: What Is the Mechanism for Spin-Coupling?

Min Zhao,[†] Chang Zhong,[†] Charlotte Stern,[†] Anthony G. M. Barrett,*[,‡] and Brian M. Hoffman*[,†]

Contribution from the Departments of Chemistry, Northwestern University, Evanston, Illinois 60208-3113, and Imperial College of Science, Technology, & Medicine, London SW7 2AY, U.K.

Received October 11, 2004; E-mail: agmb@ic.ac.uk; bmh@northwestern.edu

Abstract: Dimetallic Schiff base−porphyrazine (pz) compounds, denoted **1**[M^1; M^2; R], have been prepared, where metal ion M^1 is incorporated into the pz core, and metal ion M^2 is bound to a bis(5-*tert*-butylsalicylidenimine) chelate built onto two amino nitrogens attached to the pz periphery; R is a solubilizing group (either propyl (Pr) or 3,4,5-trimethoxyphenyl (TMP)) attached to the remaining carbons of the pz periphery. The synthesis of **1**[Cu; Cu; R], **1**[Cu; VO; R], **1**[ClMn; Cu; Pr], and **1**[ClMn; VO; Pr] is discussed, the crystal structures of **1**[Cu; Cu; TMP] and **1**[ClMn; VO; Pr] are presented, and the magnetic properties of these compounds are compared. The pattern of ligand-mediated exchange coupling in these complexes is startling: for the Cu−M^2 complexes **1**[Cu; VO; R] and **1**[Cu; Cu; R], $2 \times 10^2 \leq |J(\text{Cu}-\text{VO})/J(\text{Cu}-\text{Cu})|$; for the ClMn−$M^2$ complexes **1**[ClMn; Cu; Pr] and **1**[ClMn; VO; Pr], $J(\text{ClMn}-\text{VO})/J(\text{ClMn}-\text{Cu}) \approx 1/3$, an inverse ratio from that of the Cu−M^2 complexes, but with lesser discrimination. This coupling pattern is explained in terms of a novel orientation relative to the M^1-M^2 direction: the "square-planar" Schiff base ligand set of M^2 is rotated in-plane by 45° relative to the effectively coplanar pz ligand set of M^1.

Introduction

Magneto-structural studies of the interactions between metal centers in spin-coupled dimetallic systems are a foundation of efforts to generate high-spin molecules. Homobinuclear complexes of copper(II) have been intensively used to derive magneto-structural correlations: according to a recent review, more than 900 of such complexes have been structurally characterized.[1] Only a few heterobinuclear complexes have been synthesized because of the relative difficulty of their synthesis. In general, such heterobimetallic compounds have involved a metal complex as a ligand for a simple metal salt,[2−4] or the stepwise reaction of a ligand having two different coordination sites with two different metal ions.[5,6]

Porphyrazines (pz's) have been shown to be a template to rigidly organize multiple metal ions. The unique synthetic route of porphyrazine, by template cyclization of maleonitrile derivatives, allows us to prepare pz's with a variety of peripheral groups, especially with S, N, or O heteroatom peripheral functionalization, and to bind metal ions at the periphery through the heteroatoms.[7−15] We have developed a new type of binucleating ligand, porphyrazines with a Schiff base appended to the periphery, and reported the synthesis of dimetallic compounds M^1[pz]−M^2[Schiff base].[16]

To define the systematics of spin-coupling within the Schiff base−porphyrazine system, herein we present the synthesis and characterization of binuclear Cu(II)−Cu(II), Cu(II)−VO(II), ClMn(III)−Cu(II), and ClMn(III)−VO(II) compounds, **1**[M^1; M^2; R] (Chart 1), derived from this ligand system. We report a surprising pattern to the strength of spin-coupling, and explain

[†] Northwestern University.
[‡] Imperial College of Science, Technology, & Medicine.

(1) Melnik, M.; Kabesova, M.; Koman, M.; Macaskova, L.; Garaj, J.; Holloway, C. E.; Valent, A. *J. Coord. Chem.* **1998**, *45*, 147−359.
(2) Kahn, O.; Tola, P.; Galy, J.; Coudanne, H. *J. Am. Chem. Soc.* **1978**, *100*, 3931−3933.
(3) Cortes, R.; Urtiaga, M. K.; Lezama, L.; Arriortua, M. I.; Rojo, T. *Inorg. Chem.* **1994**, *33*, 829−832.
(4) O'Connor, C. J.; Freyberg, D. P.; Sinn, E. *Inorg. Chem.* **1979**, *18*, 1077−1088.
(5) Tomlonovic, B.; Hough, R. L.; Glick, M. D.; Lintvedt, R. L. *J. Am. Chem. Soc.* **1975**, *97*, 2925−2927.
(6) Lintvedt, R. L.; Glick, M. D.; Tomlonovic, B. K.; Gavel, D. P. *Inorg. Chem.* **1976**, *15*, 1646−1654.
(7) Velázquez, C. S.; Fox, G. A.; Broderick, W. E.; Andersen, K. A.; Anderson, O. P.; Barrett, A. G. M.; Hoffman, B. M. *J. Am. Chem. Soc.* **1992**, *114*, 7416−7424.
(8) Velázquez, C. S.; Baumann, T. F.; Olmstead, M. M.; Hope, H.; Barrett, A. G. M.; Hoffman, B. M. *J. Am. Chem. Soc.* **1993**, *115*, 9997−10003.
(9) Baumann, T. F.; Nasir, M. S.; Sibert, J. W.; White, A. J. P.; Olmstead, M. M.; Williams, D. J.; Barrett, A. G. M.; Hoffman, B. M. *J. Am. Chem. Soc.* **1996**, *118*, 10479−10486.
(10) Michel, S. L. J.; Goldberg, D. P.; Stern, C. L.; Barrett, A. G. M.; Hoffman, B. *J. Am. Chem. Soc.* **2001**, *123*, 4741−4748.
(11) Goldberg, D. P.; Michel, S. L. J.; White, A. J. P.; Williams, D. J.; Barrett, A. G. M.; Hoffman, B. M. *Inorg. Chem.* **1998**, *37*, 2100−2101.
(12) Goldberg, D. P.; Montalban, A. G.; White, A. J. P.; Williams, D. J.; Barrett, A. G. M.; Hoffman, B. M. *Inorg. Chem.* **1998**, *37*, 2873−2879.
(13) Lange, S. J.; Nie, H.; Stern, C. L.; Barrett, A. G. M.; Hoffman, B. M. *Inorg. Chem.* **1998**, *37*, 6435−6443.
(14) Zhao, M.; Stern, C.; Barrett, A. G. M.; Hoffman, B. M. *Angew. Chem., Int. Ed.* **2003**, *42*, 462−465.
(15) Cook, A. S.; Williams, D. B. G.; White, A. J. P.; Williams, D. J.; Lange, S. J.; Barrett, A. G. M.; Hoffman, B. M. *Angew. Chem., Int. Ed.* **1997**, *36*, 760−761.
(16) Zhao, M.; Zhong, C.; Stern, C.; Barrett, A. G. M.; Hoffman, B. M. *Inorg. Chem.* **2004**, *43*, 3377−3385.

Chart 1

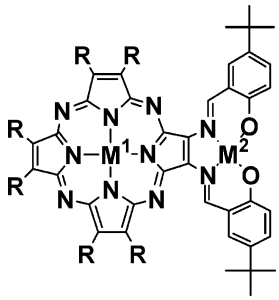

1[M^1; M^2; R]

it with an analysis based on the fact that the metal ligands of the pz and Schiff base have a novel orientation relative to the M−M direction: the "square-planar" ligand set of M^2 is rotated in-plane by 45° relative to the effectively coplanar ligand set of M^1.

Experimental Section

Materials and Methods. All starting materials were purchased from Aldrich Chemical and used as received, with the exception of vanadium(IV) oxide bis(2,4-pentanedionate) ($VO(acac)_2$), which was purchased from Alfa Aesar and used as received. All solvents were used as supplied. Silica gel used for chromatography was Whatman silica gel 60 Å (230−400 mesh) from VWR. Porphyrazines **2**[Cu; Pr],[16] **2**[Cu; TMP],[16] **2**[Mg; Pr],[17] and **1**[ClMn; Cu; Pr][14,16] were prepared as previously reported. [*N*,*N*′-Ethylenebis(salicylideneaminate)]copper(II)[18] and [*N*,*N*′-ethylenebis(salicylideneaminate]oxovanadium(IV)[19] were prepared and purified as described previously. Schlenk-line manipulations were performed on an apparatus purchased from Chemglass and with dry nitrogen.

Electronic absorption spectra were recorded using a Hewlett-Packard HP8452A diode array spectrophotometer. Fast atom bombardment mass spectra (FAB-MS) were recorded by the Mass Spectrometry Laboratory in University of Illinois at Urbana−Champaign. Atmospheric-phase chemical ionization mass spectra (APCI-MS) and electrospray ionization mass spectra (ESI-MS) were recorded using a Finnigan LCQ Advantage mass spectrometer. Electron paramagnetic resonance (EPR) spectra were measured by using a modified Varian E-4 X-band spectrometer. Solid-state magnetic susceptibility measurements were made for a polycrystalline sample by using a Quantum Design MPMS SQUID susceptometer operating in the temperature range 2−300 K and with a 500 H magnetic field.

Cu[Pz(A; B_3)], A = Copper(II) Bis(5-*tert*-butylsalicylidenimine), B = (*n*-Propyl)$_2$, 1[Cu; Cu; Pr]. H_2S was bubbled into a suspension of **2**[Cu; Pr] in anhydrous pyridine with 50-fold excess 5-*tert*-butyl-2-hydroxybenzaldehyde for 10 min, during which time the solid was totally dissolved and the blue solution turned to bluish purple. The solvent was then removed under reduced pressure. The remaining solid was washed with methanol until the eluate was colorless and then dissolved in chloroform and methanol (4:1). Anhydrous $CuCl_2$ (10-fold) was added, and the reaction was stirred at room temperature overnight. The desired product was separated through column chromatography with chloroform and dried as a blue powder. Yield: 50%. UV−vis (CH_2Cl_2): λ_{max} 346, 600, 666. FAB-MS: *m*/*z* 1039.6 (M + H^+), calcd for $C_{56}H_{69}N_{10}O_2Cu_2$ 1039.4.

Cu[Pz(A; B_3)], A = Copper(II) Bis(5-*tert*-butylsalicylidenimine), B = (3,4,5-Trimethoxyphenyl)$_2$, 1[Cu; Cu; TMP]. Compound **2**[Cu; TMP] and 50-fold excess 5-*tert*-butyl-2-hydroxybenzaldehyde were put into a three-neck round-bottom flask, 20 mL of anhydrous pyridine was added via syringe, and H_2S was bubbled through the reaction mixture for 5 min, during which time the blue solution turned to bluish purple. The solvent was evaporated under reduced pressure, and the residue was chromatographed using 4% methanol in chloroform. Without further purification, the crude ligand was dissolved in 20 mL of methanol and 20 mL of chloroform, with the addition of 10-fold excess anhydrous $CuCl_2$ and trace amounts of triethylamine. The reaction was brought to reflux for 2 h until there was no further change in the UV−vis spectra. The expected product was then purified by column chromatography (4% methanol in methylene chloride). Yield: 45%. UV−vis (CH_2Cl_2): λ_{max} 349, 532, 645. ESI-MS: *m*/*z* 1785.7 (M + H^+), calcd for $C_{92}H_{93}N_{10}O_{20}Cu_2$ 1785.9.

Cu[Pz(A; B_3)], A = Vanadium(II) Oxide-bis(5-*tert*-butylsalicylidenimine), B = (*n*-Propyl)$_2$, 1[Cu; VO; Pr]. The compound was prepared using the same procedure as for **1**[Cu; Cu; Pr]. Yield: 54%. UV−vis (CH_2Cl_2): λ_{max} 339, 592, 654. APCI-MS: *m*/*z* 1043.4 (M + H^+), calcd for $C_{56}H_{69}N_{10}O_3CuV$ 1043.4.

Cu[Pz(A; B_3)], A = Vanadium(II) Oxide-bis(5-*tert*-butylsalicylidenimine), B = (3,4,5-Trimethoxyphenyl)$_2$, 1[Cu; VO; TMP]. This compound was synthesized by a procedure similar to that used for **1**[Cu; Cu; TMP], except that NaOMe was used as the base and the reaction was stirred at room temperature overnight. Yield: 43%. UV−vis (CH_2Cl_2): λ_{max} 348, 537, 679. APCI-MS: *m*/*z* 1788.4 (M + H^+), calcd for $C_{92}H_{93}N_{10}O_{21}CuV$ 1788.5.

ClMn[Pz(A; B_3)], A = Vanadium(II) Oxide-bis(5-*tert*-butylsalicylidenimine), B = (*n*-Propyl)$_2$, 1[ClMn; VO; Pr]. H_2S was bubbled through a solution of **2**[Mg; Pr] (28.0 mg, 0.0403 mmol) and 5-*tert*-butyl-2-hydroxybenzaldehyde (353 mg, 50-fold excess) in 10 mL of pyridine for 5 min, during which time the blue color changed to violet. The solvent was evaporated, and the residue was purified via column chromatography in 4% methanol in chloroform (with 0.5% triethylamine) and then redissolved in methanol. Ten equivalent of VO(acac) and trace amount of triethylamine were then added. The reaction was stirred at room temperature overnight. The solvent was then evaporated, and column chromatography was applied. The major blue fraction was collected and dissolved in 10 mL of DMF and 20 mL of chlorobenzene. Excess $MnCl_2$ (10-fold) was added, and the reaction was brought to 100 °C; it was stopped when there were no further changes in the optical spectrum. The solvent was evaporated, the residue was dissolved in methylene chloride, and the solution was stirred with brine for 30 min. The organic phase was separated, and column chromatography (4% methanol in methylene chloride) afforded the green product, 20.1 mg. Yield: 46.6%. UV−vis (CH_2Cl_2): λ_{max} 337, 382, 573, 642, 685. FAB-MS: *m*/*z* 1035.4 (M − Cl)$^+$, calcd $C_{56}H_{68}N_{10}O_3MnV$ 1035.1.

X-ray Structure Determination. A summary of the crystal data and structure refinement parameters for compound **1**[Cu; Cu; TMP] and **1**[ClMn; VO; Pr] is provided in Table 1. Both structures were solved by direct methods and expanded using Fourier techniques and were refined by full-matrix least-squares based on F^2. All of the non-hydrogen atoms of both complexes were refined anisotropically. Hydrogen atoms were included but not refined. For **1**[Cu; Cu; TMP], a structural model consisting of the host molecule plus disordered solvate molecules was developed; since positions for the solvate molecules were poorly determined, a second structural model was refined with contributions from the solvate molecules removed from diffraction data using the bypass procedure in PLATON (Spek, 1990). No positions for the host network differed by more than two significant units between these two refined models. The electron count from the "squeeze" model converged to 897 electrons in a total potential solvent-accessible area volume of 3176.7 Å^3. For **1**[ClMn; VO; Pr], the other disordered components to C24, C31, and C34 were not found in the

(17) Baum, S. M.; Trabanco, A. A.; Andres, A.; Montalban, A.; Micallef, A. S.; Zhong, C.; Meunier, H. G.; Suhling, K.; Phillips, D.; White, A. J. P.; Williams, D. J.; Barrett, A. G. M.; Hoffman, B. M. *J. Org. Chem.* **2003**, *68*, 1665−1670.
(18) Bhadbhade, M. M.; Srinivas, D. *Inorg. Chem.* **1993**, *32*, 6122−6130.
(19) Bonadies, J. A.; Carrano, C. J. *J. Am. Chem. Soc.* **1986**, *108*, 4088−4095.

Table 1. Crystallographic Data for **1**[Cu; Cu; TMP] and **1**[ClMn; VO; Pr][a]

	1[Cu; Cu; TMP]	**1**[ClMn; VO; Pr]
empirical formula	$C_{92}H_{92}N_{10}O_{20}Cu_2$	$C_{55}H_{63.25}N_{10.25}O_3MnVCl$
formula weight	1784.84	1057.25
crystal size/mm	0.316 × 0.302 × 0.142	0.428 × 0.344 × 0.144
lattice type	monoclinic	triclinic
space group	$P2_1/n$	$P\bar{1}$
a/Å	13.959(3)	11.1722(17)
b/Å	42.297(15)	13.105(2)
c/Å	18.391(5)	19.514(3)
α/deg	90	92.328(2)
β/deg	94.814(18)	98.748(2)
γ/deg	90	94.309(3)
V/Å^3	10820(5)	2812.0(7)
Z, D_c/g cm^{-3}	4, 1.095	2, 1.253
absorption coefficient/mm^{-1}	0.455	0.489
F(000)	3728	1112
θ range for data collection/deg	1.21−29.20	1.56−28.97
reflections collected/unique	96 607/26 468 [R(int) = 0.1309]	25 165/13 127 [R(int) = 0.0389]
completeness to θ_{max}/%	90.3	88.0
absorption correction	none	integration
data/restraints/parameters	26 468/0/1141	13 127/0/694
goodness-of-fit on F^2	0.945	1.087
R_1[b]	0.1137	0.0818
wR_2[c]	0.2812	0.2388

[a] Details in common: graphite-monochromated Mo Kα radiation, wavelength 0.71073 Å, Bruker SMART-1000 CCD area detector, 153(2) K, full-matrix least-squares refinement based on F^2. [b] $R_1 = \sum||F_o| - |F_c||/\sum|F_o|$. [c] $wR_2 = [\sum(w(F_o^2 - F_c^2)^2)/\sum w(F_o^2)^2]^{1/2}$.

difference map. A group anisotropic displacement parameter was refined for the disordered C25 atom. The solvent atom was refined to quarter occupancy.

Results and Discussions

Synthesis. The preparation of porphyrazines **1**[Cu; M^2; R] begins with the reductive deselenation of **2**[Cu; R] in pyridine by hydrogen sulfide to form a free amino group terminal (Scheme 1), a strategy developed by Ercolani et al.[20] In the presence of a large excess of 5-*tert*-butyl-2-hydroxybenzaldehyde (50-fold), the condensation reaction between the carbonyl group and the amino group leads to **3**[Cu; 2H; R], which reacts with metal salts to give the dimetallic Schiff base pz's. The availability of both R = *n*-propyl (Pr) and R = 3,4,5-trimethoxyphenyl (TMP) groups as substituents on the other pyrroles allows us to optimize solubility: compounds **1**[ClMn; M^2; Pr] are soluble in organic solvents and solutions of these are readily studied, while compounds **1**[Cu; M^2; Pr] are not. In contrast, compounds **1**[Cu; M^2; TMP] are readily soluble in most common organic solvents.

The preparation of compound **1**[ClMn; VO; Pr] started from **2**[Mg; Pr] instead of **1**[ClMn; Pr] (Scheme 2), because of the sensitivity of Mn(III) to basic conditions. Deprotection (H_2S, pyridine)[14,16,20] of **2**[Mg; Pr] in the presence of 5-*tert*-butyl-2-hydroxybenzaldehyde afforded the ligand **3**[2H; 2H; Pr]. Sequential metalation of VO(II) in the reactive peripheral Schiff base and ClMn(III) in the porphyrazine core gave the target compound, **1**[ClMn; VO; Pr].

X-ray Structure of 1[Cu; Cu; TMP]. Dark blue, platelike crystals of **1**[Cu; Cu; TMP] were grown from ethyl acetate/methanol solution. The crystal structure is illustrated in Figure 1, and bond distances and angles relevant to the copper coordination sphere are listed in Table 2. The Cu(1) in the pz core adopts an essentially square-planar coordination geometry: the four Cu−N bonds lie between 1.926 and 1.937 Å, and the four N−Cu−N angles are in the range of 89.48°−90.31°. The structure of the Cu(2) ion in the Schiff base site closely resembles that of [Cu(5-CH_3O-salen)].[18] The copper and its coordinating atoms are planar, with the sum of angles at copper equalling 360.1° and Cu displaced by only 0.0252 Å from the least-squares N_2O_2 plane (mean deviation of all atoms from the plane is 0.047 Å). The major difference in the two similar structures is the dimension of the Cu−NCCN chelate ring. C(14)−N(9) and C(91)−N(10) (1.365(7) and 1.373(6) Å, respectively) are much shorter in **1**[Cu; Cu; TMP] than the equivalent bonds in [Cu(5-CH_3O-salen)] (1.47(2) and 1.49(1) Å, respectively). Also the C(14)−C(91) bond (1.397(7) Å) within the pz conjugated system is significantly shorter than the [Cu(5-CH_3O-salen)] C−C bond (1.49(1) Å), as expected.

X-ray Structure of 1[ClMn; VO; Pr]. A dark block crystal was grown from methylene chloride/methanol solution; Figure 2 shows the crystal structure. The manganese ion adopts a distorted square-pyramidal coordination geometry and is 0.2933 Å out of the N_4 plane (mean deviation of all atoms from the plane is 0.0394 Å), as with other ClMn(III) porphyrazines.[12,14,21] The Mn−Cl distance is 2.3408 Å, nearly the same as the value for **1**[ClMn; Cu; Pr].[14] The coordination geometry around the vanadium ion is also a distorted square pyramid. The V atom is displaced 0.5863 Å from the equatorial coordination plane N_2O_2 (planar to within 0.0148 Å), and the V=O distance is 1.591 Å. These two values are comparable with those of monomeric tetradentate Schiff base−oxovanadium(IV) complexes.[22,23]

Magnetic and EPR Studies. The EPR spectrum of **1**[Cu; Cu; Pr] in frozen solution could not be collected because of its poor solubility in organic solvents. However, the enhanced solubility of **1**[Cu; Cu; TMP] enabled us to record its 77 K spectrum dissolved in 10% chloroform/methylene chloride (Figure 3). For comparison, the figure includes a spectrum of a solid powder of **2**[Cu; Pr] magnetically diluted in its free-base diamagnetic host as a model for the copper core of **1**[Cu; Cu; TMP]; for a model of the peripheral copper, the figure includes the spectrum of a frozen solution of a very common and well-studied copper Schiff base compound, [*N*,*N*′-ethylenebis(salicylideneaminate)]copper(II) (Cu(salen)). The EPR spectrum of **2**[Cu; Pr] has the axial symmetry typical of monomeric square-planar Cu(II) complexes: $g_\perp = 2.05$, $g_{||} = 2.14$, $A_{||}^{Cu} = 220.0$ G.[16] The d^9 Cu(II) ion in Cu(salen) behaves quite similarly, with $g_{||} \approx 2.2$, $g_\perp \approx 2.05$, and $A_{||}^{Cu} \approx 197$ G.[24]

The EPR spectrum of the dimetallic compound **1**[Cu; Cu; TMP] is not a simple addition of the spectra of the two individual spin centers, as would be seen if the two copper units were independent. Instead, the $g_{||}$ region of the spectra shows a superposition of two seven-line hyperfine patterns. Within a pattern, the average splitting, $\bar{A}_{||}^{Cu} \approx [(A_{||}^{Cu}(pz) + A_{||}^{Cu}(Schiff\ base))/2]/2 \approx 92$ G; the two patterns are offset around $g_{||}$ by $2D/g_{||}\beta \approx 180$ G; D is the dipolar zero-field splitting parameter,

(20) Bauer, E. M.; Ercolani, C.; Galli, P.; Popkova, I. A.; Stuzhin, P. A. *J. Porphyrins Phthalocyanines* **1999**, *3*, 371−379.
(21) Ricciardi, G.; Bavoso, A.; Bencini, A.; Rosa, A.; Lelj, F.; Bonosi, F. *J. Chem. Soc., Dalton Trans.* **1996**, 2799−2807.
(22) Hoshina, G.; Tsuchimoto, M.; Ohba, S.; Nakajima, K.; Uekusa, H.; Ohashi, Y.; Ishida, H.; Kojima, M. *Inorg. Chem.* **1998**, *37*, 142−145.
(23) Ryuichi, K.; Tsuchimoto, M.; Ohba, S.; Nakajima, K.; Ishida, H.; Kojima, M. *Inorg. Chem.* **1996**, *35*, 7661−7665.
(24) Tauber, C. E.; Allen, H. C., Jr. *J. Phys. Chem.* **1979**, *83*, 1391−1393.

Scheme 1. Synthesis of **1**[Cu; M^2; R]

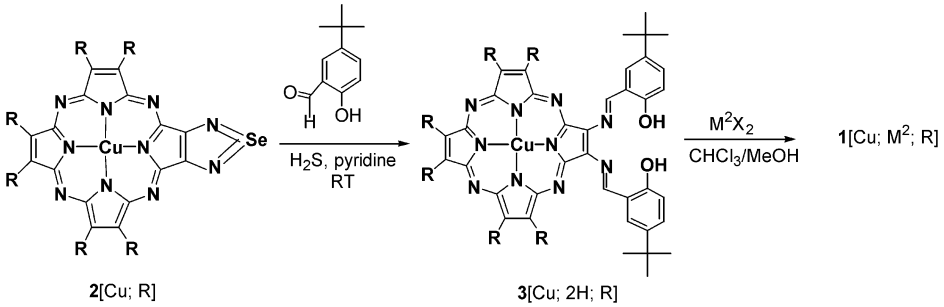

Scheme 2. Synthesis of **1**[ClMn; VO; Pr]

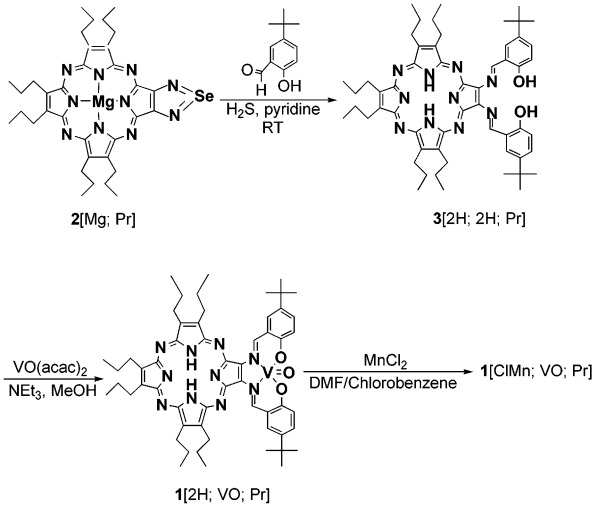

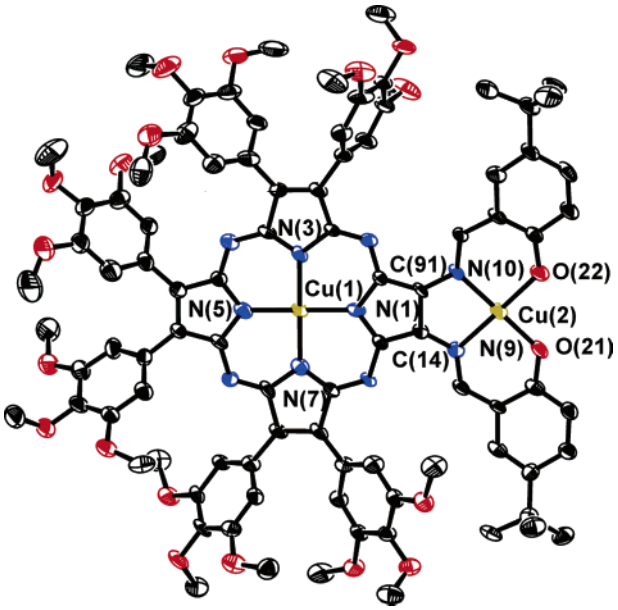

Figure 1. X-ray structure of **1**[Cu; Cu; TMP].

and its value is close to that expected for the dipole−dipole interaction.[25] This spectrum indicates that the two Cu(II) centers experiences a Heisenberg exchange coupling (eq 1), with $|J| \gg g\beta\bar{A}$.

The exchange interaction between the two single-ion spin

(25) Bencini, A.; Gatteschi, D. *Electron Paramagnetic Resonance of Exchange Coupled Systems*; Springer-Verlag: Berlin, Heidelberg, New York, 1990.

Table 2. Interatomic Distances (Å) and Angles (deg) Relevant to the Copper Coordination Sphere in **1**[Cu; Cu; TMP]

Cu(1)−N(1)	1.926(5)	Cu(1)−N(3)	1.933(5)
Cu(1)−N(5)	1.930(5)	Cu(1)−N(7)	1.937(5)
Cu(2)−O(21)	1.899(4)	Cu(2)−O(22)	1.904(4)
Cu(2)−N(9)	1.973(5)	Cu(2)−N(10)	1.948(5)
C(14)−N(9)	1.365(7)	C(91)−N(10)	1.373(6)
C(14)−C(91)	1.397(7)		
N(1)−Cu(1)−N(3)	89.48(18)	N(1)−Cu(1)−N(7)	89.92(19)
N(5)−Cu(1)−N(3)	90.31(19)	N(5)−Cu(1)−N(7)	90.2(2)
N(1)−Cu(1)−N(5)	179.1(2)	N(3)−Cu(1)−N(7)	175.5(2)
O(21)−Cu(2)−O(22)	88.08(16)	O(21)−Cu(2)−N(9)	93.26(17)
O(22)−Cu(2)−N(10)	93.31(17)	N(10)−Cu(2)−N(9)	85.45(18)
O(21)−Cu(2)−N(10)	175.49(19)	O(22)−Cu(2)−N(9)	178.17(19)

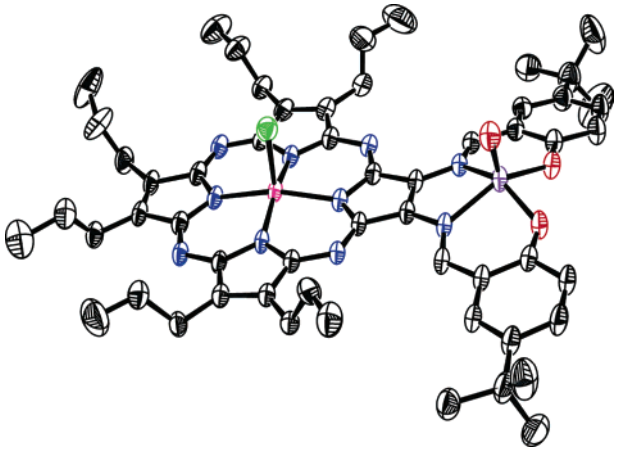

Figure 2. X-ray structure of **1**[ClMn; VO; Pr].

$$\hat{H} = JS_1 \cdot S_2 \qquad (1)$$

doublets splits the spin manifold into states with total spin of $S = 0$ and $S = 1$, separated by J; for positive J the spin triplet is the higher level. To determine J, the temperature dependence of the magnetic susceptibility for complex **1**[Cu; Cu; Pr] was measured (Figure 4). The susceptibility monotonically increases with decreasing the temperature in the range of 300 to 2 K, and the plot of the χ_m vs T is well described by the Curie−Weiss law: $\chi_m = B + C/(T - \Theta)$, with $B = -0.00566$ cm^3/mol, $C = 0.808$ (cm^3 K)/mol, and $\Theta = -1.00$ K. Compound **1**[Cu; Cu; TMP] shows the same magnetic behavior as **1**[Cu; Cu; Pr], and the Curie−Weiss law fit gives $B = -0.00988$ cm^3/mol, $C = 0.796$ (cm^3 K)/mol, and $\Theta = -0.08$ K, where the Weiss constant, Θ, corresponds to the sum of intra- and intermolecular exchange between spins. Thus we have very weak Cu−Cu coupling in **1**[Cu; Cu; R]: $g\beta\bar{A}/k_B \ll |J|/k_B \ll |\Theta| = 0.08$ K. The value is too small to decide whether the coupling is antiferromagnetic or ferromagnetic, but in either

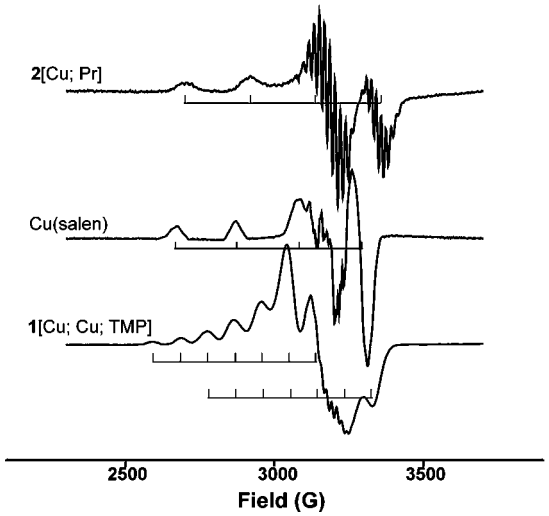

Figure 3. X-band EPR spectra of **2**[Cu; Pr], Cu(salen), and **1**[Cu; Cu; TMP].

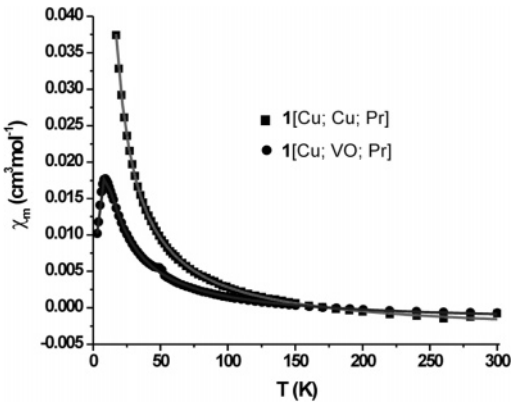

Figure 4. Plot of the molar magnetic susceptibility of a powdered sample of **1**[Cu; Cu; Pr] (■) and **1**[Cu; VO; Pr] (●) versus temperature. The solid lines are a fit by Curie−Weiss law to **1**[Cu; Cu; Pr], $B = -0.00566$ cm^3/mol, $C = 0.808$ (cm^3 K)/mol, $\Theta = -1.00$ K, and a fit to **1**[Cu; VO; Pr] by eq 1, $g = 2.03$, $J/k_B = 13.8$ K, $\rho = 0.07$, $N\alpha = -0.00213$ cm^3 mol^{-1}, $\Theta = -2.33$ K.

case, it is negligible. This result is different from that obtained for the previously reported binuclear copper complexes: in most of those cases there is a strong antiferromagnetic coupling between the two copper ions.[26−31]

Again, we could not record the frozen-solution EPR spectrum of **1**[Cu; VO; Pr] because of the poor solubility, but **1**[Cu; VO; TMP] dissolved well in 10% chloroform/dichloromethane and afforded a good EPR spectrum in frozen solution at 77 K (Figure 5). The figure displays the reference spectra of **2**[Cu; Pr] and [*N*,*N*′-ethylenebis(salicylideneaminate)]oxovanadium(IV) (VO(salen)); the spin-Hamiltonian parameters of VO(salen) in frozen solution are $g_\perp = 1.985$, $g_{||} = 1.951$, $|A_\perp| = 59 \times 10^{-4}$ cm^{-1}, and $|A_{||}| = 159 \times 10^{-4}$ cm^{-1}. The spectrum of **1**[Cu; VO; TMP] is complicated by hyperfine splittings from exchange-coupled ^{51}V and ^{63,65}Cu centers, which again shows a coupling where $J \gg g\beta\bar{A}$, along with a zero-field splitting interaction.

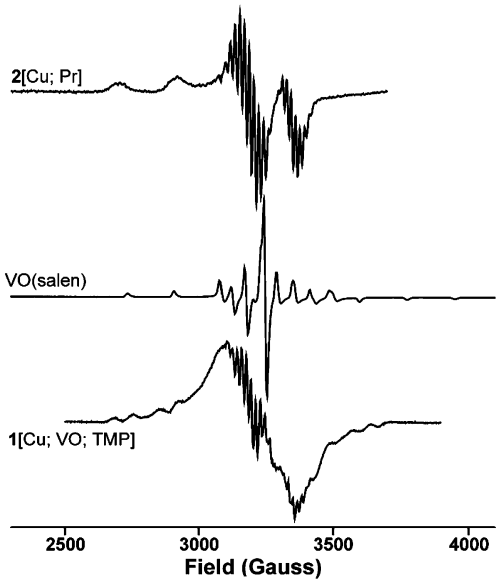

Figure 5. X-band EPR spectra of 2[Cu; Pr], VO(salen), and 1[Cu; Cu; TMP].

Variable-temperature susceptibility measurements were carried out on **1**[Cu; VO; Pr] and **1**[Cu; VO; TMP]. The experimental data for **1**[Cu; VO; Pr] are illustrated in Figure 4; it shows a sharp maximum in χ_m at ∼8 K, the result of antiferromagnetic Cu−VO exchange coupling. The data were fit to the Bleaney−Bowers equation (eq 2)[32] for exchange-coupled pairs of Cu(II) and VO(II) ions on the basis of the isotropic exchange Hamiltonian (eq 1) for two interacting $S = {}^1/_2$ centers.

$$\chi_m = \frac{N\beta^2 g^2}{3k_B(T-\Theta)}\left[1+\frac{1}{3}\exp(J/k_BT)\right]^{-1}(1-\rho) + \frac{[N\beta^2 g^2]\rho}{4k_BT} + N\alpha \quad (2)$$

In eq 2, χ_m is expressed as cubic centimeters kelvin per mole of M(II) ion; the Curie term allows for a fraction of monomeric impurity spins ρ, while $N\alpha$ describes the temperature-independent susceptibility. To account for possible interdimer magnetic interactions, a Weiss-like correction term Θ is introduced; the other parameters have their usual meaning. The solid lines correspond to the best fit of the data for **1**[Cu; VO; Pr] to eq 2: $g = 2.03$, $J/k = 13.8$ K, $\rho = 0.07$, $N\alpha = -0.00213$ cm^3 mol^{-1}, $\Theta = -2.33$ K. For **1**[Cu; VO; TMP], $g = 2.01$, $J/k_B = 12.5$ K, $\rho = 0.11$, $N\alpha = -0.00059$ cm^3 mol^{-1}, and $\Theta = -4.02$ K. Thus, the ratio of Cu−M^2 coupling constants for M^2 = VO, Cu is extraordinarily large: if J(Cu−Cu) is antiferrromagnetic, $2 \times 10^2 \leq |J(\text{Cu−VO})/J(\text{Cu−Cu})|$.

X-band EPR spectra of **1**[ClMn; Cu; Pr] and **1**[ClMn; VO; Pr] taken at 77 K are shown in Figure 6. As we discussed previously, both the spectra of **1**[ClMn; Cu; Pr][14,16] and **1**[ClMn; VO; Pr] are the result of strong Heisenberg exchange coupling between the $S = 2$ and $S = {}^1/_2$ spins, which produces two total-spin manifolds with $S = {}^3/_2$ and ${}^5/_2$, separated by $\Delta = 5J$. Both spectra show "perpendicular" features at $g_\perp \approx 6$ and $g_\perp \approx 4$, the former characteristic of the $S = {}^5/_2$ spin state, the latter of the $S = {}^3/_2$ state, both with axial zero-field splitting (zfs)

(26) Kogan, V. A.; Lukov, V. V. *Russ. J. Coord. Chem.* **2004**, *30*, 205−213.
(27) Melnik, M. *Coord. Chem. Rev.* **1982**, *42*, 259−293.
(28) Hasty, E. F. W.; Lon, J.; Hendrickson, D. N. *Inorg. Chem.* **1978**, *17*, 1834−1841.
(29) Lambert, S. L. H.; David, N. *Inorg. Chem.* **1979**, *18*, 2683−2686.
(30) Thompson, L. K. T.; Santokh, S. *Comm. Inorg. Chem.* **1996**, *18*, 125−144.
(31) Thompson, L. K.; Mandal, S. K.; Tandon, S. S.; Bridson, J. N.; Park, M. K. *Inorg. Chem.* **1996**, *35*, 3117−3125.
(32) Bleaney, B. B., K. D. *Proc. R. Soc. London* **1952**, 451.

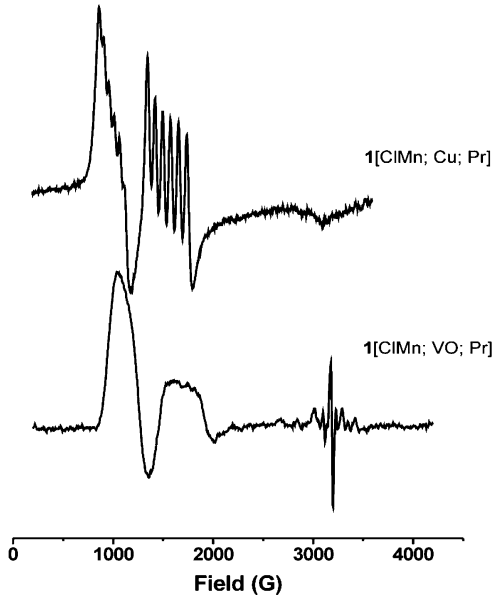

Figure 6. X-band EPR spectra of 1[ClMn; Cu; Pr] and 1[ClMn; VO; Pr].

parameter (*DS*) large compared to the microwave quantum.[33] The spectrum of **1**[ClMn; Cu; Pr] shows resolved sextet hyperfine patterns from interaction with ^{55}Mn($I = {}^5/_2$) in both $g_\perp \approx 4$ and $g_\perp \approx 6$ features: $A_{Mn}{}^{3/2} = (6/5)A_{Mn} = 80$ G, $A_{Mn}{}^{5/2} = (4/5)A_{Mn} = 53$ G, and A_{Mn} is the intrinsic value for the uncoupled Mn(III) ($S = 2$) ion. The ^{55}Mn splitting patterns are clearly present but unresolved in **1**[ClMn; VO; Pr]. The spectrum of **1**[ClMn; Cu; Pr] further shows unresolved intensity from the associated $g_{||}$ features around $g = 2$, that from **1**[ClMn; VO; Pr] must do so as well, but the region is partially obscured by a signal from impurity vanadyl ion.

The difference in the resolution of the M^2 = Cu and M^2 = VO complexes is caused by unresolved hyperfine splittings from M^2. Simple calculation shows[14] that the M^2 hyperfine coupling is sharply reduced in the total-spin manifolds generated by the spin exchange: $A_\perp(M^2)^{3/2} = A_\perp(M^2)^{5/2} = \pm(1/5)A_\perp(M^2)$. Each line of the Mn sextet of **1**[ClMn; Cu; Pr] must contain the hyperfine splitting of Cu ($I = {}^3/_2$), which would broaden the line by about $(2I)A_\perp{}^S = 3\ A_\perp{}^S = 3/5\ A_\perp$(Cu). As $A_\perp$(Cu) $\approx$ 30 G is small, the broadening by Cu is small, and the sextet from ^{55}Mn is well resolved. Likewise for **1**[ClMn; VO; Pr], $A_\perp(VO)^{3/2} = A_\perp(VO)^{5/2} = \pm(1/5)A_\perp$(VO), but in this case the V ($I = {}^7/_2$) broadens the Mn lines by $(2I)A_\perp{}^S = 7\ A_\perp{}^S = 7/5\ A_\perp$(V). As $A_\perp$(V) $\approx$ 70 G, the broadening is appreciable and the Mn sextet no longer is resolved.

The observation of both signals at 77 K implies a thermal population of the two spin manifolds at this temperature. In **1**[ClMn; VO; Pr], the $S = {}^5/_2$ signal is more intense than that of $S = {}^3/_2$ compared with compound **1**[ClMn; Cu; Pr], which indicates that the *J* value is smaller for the M^2 = VO complex. We previously reported that $\Delta/k_B = 23$ K for **1**[ClMn; Cu; Pr].[14] To determine the exchange parameter Δ in **1**[ClMn; VO; Pr], the magnetic susceptibility was measured over the temperature range from 2 to 300 K using a SQUID magnetometer (Figure 7). The high-temperature limiting value, $\chi T \approx 3.2$ cm^3 mol^{-1} K, is consistent with the presence of $S = 2$ and $S = {}^1/_2$ partner

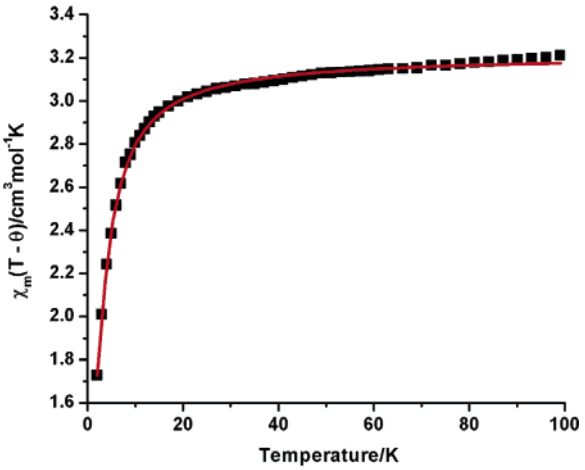

Figure 7. Plot of the molar magnetic susceptibility of a powdered sample of **1**[ClMn; VO; Pr], plotted as (χT). The solid line is a fit to the data by eq 2, with $\theta = 0.18$ K, $g = 1.95$, $D^{3/2} = (3/5)D^{Mn} = -1.38$ cm^{-1}, and $\Delta/k_B = 7$ K.

spins, each having intrinsic *g* values of 1.95. The temperature dependence of $\chi(T)$ was fit to eq 3,

$$\chi = \chi^{3/2}\frac{2}{2+3\,e^{-\Delta/k_BT}} + (C/4)\frac{35\,e^{-\Delta/k_BT}}{2+3\,e^{-\Delta/k_BT}} \qquad (3)$$

$$\chi^{3/2} = C\left[\frac{1}{3}\frac{1+9\,e^{-2D^{3/2}/k_BT}}{4(1+e^{-2D^{3/2}/k_BT})} + \frac{2}{3}\frac{4+\frac{3k_BT}{D^{3/2}}(1-e^{-2D^{3/2}/k_BT})}{4(1+e^{-2D^{3/2}/k_BT})}\right]$$

where $C = N\beta^2g^2/k_B(T-\theta)$ and the symbols have their usual meanings. The function $\chi^{3/2}$ is associated with the $S = {}^3/_2$ manifold and incorporates the effects of the zero-field splitting: $D^{3/2} = (3/5)D^{Mn}$, where $D^{Mn} = -2.3$ cm^{-1}.[34] The fits give $\Delta/k_B = 7$ K and the Curie−Weiss constant, $\theta = 0.18$ K. Thus, the ratio of ClMn−M^2 exchange parameters, J(ClMn−VO)/J(ClMn−Cu) $\approx$ 1/3, is an inverse behavior from that of the Cu−M^2 complexes, and with a lesser discrimination.

Mechanism of the Exchange Coupling. We have seen that when an M^1 = Cu(II) ion is in the pz core, the coupling with an M^2 = Cu(II) ion at the periphery is extremely weak compared to the coupling with an M^2 = VO(II) ion at the periphery: $2 \times 10^2 \le |J(\text{Cu}-\text{VO})/J(\text{Cu}-\text{Cu})|$. Conversely, when M^1 = ClMn-(III) ion is in the core, the intramolecular interaction is stronger to M^2 = Cu at the periphery: J(ClMn−VO)/J(ClMn−Cu) $\approx$ 1/3, but the discrimination between the M^2 = Cu, VO is not as great. This dramatic difference can be explained by considering the relative symmetries of the "magnetic orbitals", the d_σ orbitals $\phi_M{}^1$ and $\phi_M{}^2$ (Figure 8), which contain the single unpaired electron of the $S = {}^1/_2$ Cu(II) and VO(II) centers and the single d_σ orbital of the $S = 2$ ClMn(III).

The magnetic orbital ϕ_{Cu} centered on a Cu(II) ion in the pz core environment is $d_\sigma = d_{x^2-y^2}$, partially delocalized over the nitrogen atoms surrounding the copper to form a σ-antibonding molecular orbital. This orbital is symmetric with regard to the *xz* mirror plane (as defined in Figure 8). However, unlike the situation in most dimetallic complexes, the "square plane" of ligands of the peripheral Schiff base is rotated by 45° relative

(33) Weltner, W., Jr. *Magnetic Atoms and Molecules*; Dover: New York, 1983; pp 266−277.

(34) Krzystek, J.; Telser, J.; Pardi, L. A.; Goldberg, D. P.; Hoffman, B. M.; Brunel, L.-C. *Inorg. Chem.* **1999**, *38*, 6121−6129.

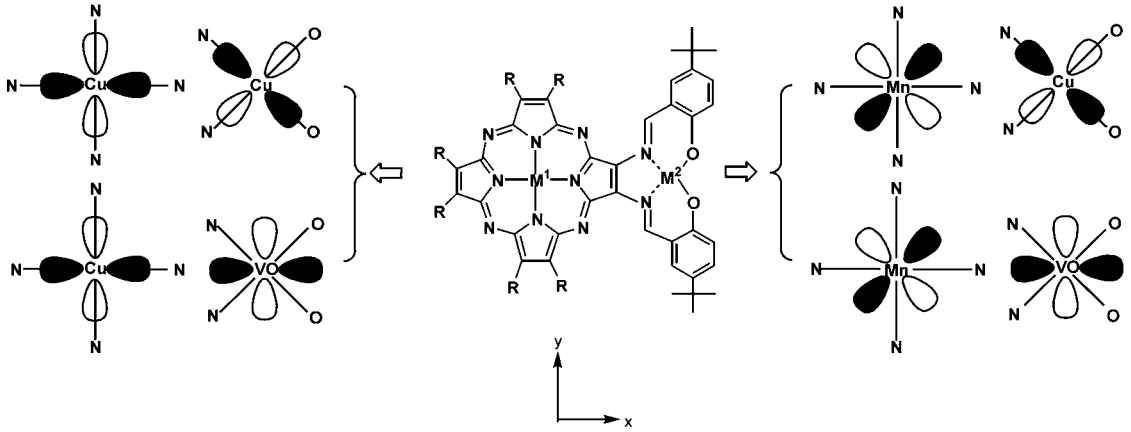

Figure 8. Relative symmetries of the magnetic orbitals in the compound pair **1**[Cu; Cu; R] and **1**[Cu; VO; R], and the compound pair **1**[ClMn; Cu; Pr] and **1**[ClMn; VO; Pr].

to that in the pz core, so the magnetic orbital $\phi_{Cu'}$ centered on the Cu(II) ion in the Schiff base is the $d_\sigma = d_{xy}$, σ-antibonding orbital, which is antisymmetric with regard to the *xz* mirror plane. Thus, $d_{\sigma(Cu)}$ and $d_{\sigma(Cu')}$ are orthogonal, and the exchange parameter *J* for the Cu−Cu pair, which is proportional to the overlap integral, $\langle\phi_{Cu}|\phi_{Cu'}\rangle$, should vanish as observed. In contrast, ϕ_{VO} is the $d_\sigma = d_{x^2-y^2}$ molecular orbital, partially delocalized over the nitrogen and oxygen ligand atoms through in-plane π-type overlap, and therefore it also is symmetric with regard to the *xz* mirror plane. Thus, while the overlap integral $\langle\phi_{Cu}|\phi_{Cu'}\rangle$ is identically zero by symmetry for the Cu(II)−Cu(II) pair, the magnetic orbitals of the Cu(II)−VO(II) pair are of the same symmetry and interact through intervening atoms. This difference in symmetry clearly underlies the large ratio of *J*(Cu−VO)/*J*(Cu−Cu) we observe.

When a high-spin d^4 M^1 = ClMn(III) ion ($S = 2$) is in the pz core, the four unpaired electrons occupy d_{xy}, d_{xz}, d_{yz}, and d_{z^2}. The only σ orbital is d_{xy}, not $d_{x^2-y^2}$ as with Cu(II), and it has the same symmetry as the magnetic orbital of the M^2 = Cu(II) ion (d_{xy}) in the Schiff base, not that of the VO(II) ion ($d_{x^2-y^2}$) in the peripheral site (Figure 8). This explains the fact that the coupling is stronger in the ClMn(III)−Cu(II) pair than the ClMn-(III)−VO(II) pair: *J*(ClMn−VO)/*J*(ClMn−Cu) ≈ 1/3.

Why is the M^2 discrimination so much less in the ClMn−M^2 complexes than in the Cu−M^2 complexes? The large discrimination between the Cu−M^2, M^2 = Cu, VO pair, $2 \times 10^2 \leq J(\text{Cu−VO})/J(\text{Cu−Cu}) \leq 10^4$, clearly indicates that the exchange involves σ-delocalization only, and that this is rigorously controlled by the symmetry constraints we have described. The dominance of σ coupling also explains the "inverse" value of the ratio, *J*(ClMn−VO)/*J*(ClMn−Cu) ≈ 1/3. However, this ratio might have been expected to have a much smaller value, $\sim 10^{-2}-10^{-4}$, if σ coupling along were operating, not 1/3. We suggest that for complexes with high-spin Mn(III), π-exchange plays a significant role: $J(\text{ClMn−M}^2) = J_\sigma(\text{ClMn−M}^2) + J_\pi(\text{ClMn−M}^2)$. When M^2 = VO, the symmetry shown in Figure 8 leads to $J_\sigma(\text{ClMn−VO}) \approx 0$, and thus $J(\text{ClMn−VO}) \approx J_\pi(\text{ClMn−VO})$; as a result, $J(\text{ClMn−VO})/J(\text{ClMn−Cu}) \approx J_\pi(\text{ClMn−VO})/([J_\sigma(\text{ClMn−Cu}) + J_\pi(\text{ClMn−Cu})]$. It is reasonable to take $J_\pi(\text{ClMn−M}^2)$ as being roughly invariant with M^2, in which case the value, $J(\text{ClMn−VO})/J(\text{ClMn−Cu}) \approx 1/3$, implies $J_\sigma(\text{ClMn−M}^2) \approx 2J_\pi(\text{ClMn−M}^2)$.

Conclusions

Two new homobinuclear Cu−Cu complexes, **1**[Cu; Cu; R], two new heterobinuclear Cu−VO complexes, **1**[Cu; VO; R], and a heterobinuclear ClMn−VO complex, **1**[ClMn; VO; Pr], have been synthesized though use of kinetic control in metal ion incorporation to Schiff base−porphyrazine ligands. **1**[Cu; Cu; TMP] and **1**[ClMn; VO; Pr] have been structurally characterized. The disposition of the ligand fields in the pz and Schiff base fragments in this system causes exchange between M^1-M^2 = Cu−Cu to be negligible compared to that in Cu−VO complexes, wherever exchange between M^1-M^2 = ClMn−Cu complex is 3-fold stronger than in ClMn−VO. The results clearly indicate that the exchange coupling for Cu and VO ions, each with a single d_σ odd electron, is rigorously controlled by the novel symmetries of the metallic orbitals and occurs through σ-delocalization. On the other hand, π-delocalization to a σ electron on M^2 from the M^1 = ClMn ($S = 2$) is deduced to be half as effective as $\sigma-\sigma$ coupling between M^1 and M^2 spins.

Acknowledgment. This work was supported by the MRSEC program of the National Science Foundation (DMR-0076097) at the materials Research Center of Northwestern University. We also thank the NSF (Grant CHE-0091364, B.M.H.) and the EPSRC (A.G.M.B.) for fundings.

Supporting Information Available: Crystallographic information files (CIF) of compounds **1**[Cu; Cu; TMP] and **1**[ClMn; VO; Pr]. This material is available free of charge via the Internet at http://pubs.acs.org.

JA0438112